Surface and Printing Properties of Synthetic Film Papers

Oswaldo J. Danella, Jr., Ruth Campomanes Santana, Sílvio Manrich, Sati Manrich

Materials Engineering Department, Materials Engineering Department, Federal University of São Carlos, Rod. Washington Luís Km 235, São Carlos SP, Brazil

Received 4 January 2002; accepted 11 July 2002

ABSTRACT: We studied the surfaces, including both the composition effects and the processing rates, of polypropylene (PP) composite films used for synthetic paper to determine the surface free energy (γ_s) and the irregularities on the film surfaces. We correlated these two characteristics to the printing quality by assessing the facility with which the offset ink was removed from the surface of the paper and also the ink absorption. Five films with different compositions were uniaxially oriented with a flat-die extruder at two different stretching rates. The results of scanning electron microscopy (SEM) of the films showed good dispersion and distribution of the filler particles used in the compositions of the films and also of the polystyrene (PS) dispersed throughout the PP matrix. The SEM analysis also revealed slightly high surface irregularities on the film surfaces through a high concentration of $CaCO_3$, which thus increased the coefficients of static and kinetic friction and the γ_s values. These film properties created better printing quality and also more strongly fixed offset ink onto the film. However, the films with high relative quantities of PS in their composition showed a high polar component in their total γ_s when compared to films with less PS or no PS in their compositions. However, because of the apolar characteristic of the offset printing ink, the ink absorption worsened. The films underwent stretching at two different rates, which did not significantly affect the γ_s values or the friction coefficients; however, they did slightly change the printing quality and ink adhesion. © 2003 Wiley Periodicals, Inc. J Appl Polym Sci 88: 2346–2355, 2003

Key words: poly(propylene) (PP); composites; polystyrene; films; surfaces

INTRODUCTION

Because of previous research into the increasing demand for cellulosic paper at international levels,[1,2] the development of synthetic paper has become the aim of several studies that have resulted in the publication of a considerable number of patents related to this product.[3–8] Furthermore, synthetic paper is practical when the inability of cellulosic paper to fulfill demand, especially in industrial printing, is considered. The positive outcome of the research related to synthetic paper validates the optimism of companies that are beginning to invest in this area.[9–11]

According to some sources, plastic films with the same characteristics as synthetic paper can be obtained by the mixture of thermoplastic polymers with filler particles, mainly, $CaCO_3$, TiO_2, and SiO_2, and/or immiscible polymer blends, such as polystyrene (PS) together with either polypropylene (PP) or polyethylene (PE).[3–5,12,13]

One of the most important characteristics of any kind of paper is its ability to be printed on. Cellulosic paper has a high capability of being printed on with several different kinds of ink because of its fibrilar and porous structures and also partially because of the high polarity of its fibers.[14–16] Several physical and chemical modifications occur during the manufacturing of cellulosic paper that also assist in printing. The addition of the filler particles and/or inorganic pigments, such as $CaCO_3$ and TiO_2, in the process modify the opacity and the mechanical properties of the paper. Furthermore, they may improve the ink absorption and the ink adhesion on the paper surface because of the hygroscopic characteristics of these filler particles.[16]

According to some authors, a very important part of improving the printing properties of synthetic paper is the development of microcavities, which is achieved by the stretching of a composite polymer film.[3,4,13] According to Benning and colleagues,[13] microcavities can be formed three different ways: (1) around the filler particles inside the main polymer, (2) in the interface of immiscible blends, or (3) between the continuous amorphous phase and the discontinuous crystalline phase of a semicrystalline polymer. This is a very important process and will produce microcavities during the stretching of the synthetic paper. Depending on which process is used, several sizes of cavities can be formed, all falling within the range 0.01–2 μm. Besides increasing ink absorption and receptivity, these cavities can also increase the opacity and decrease the density of the film, both of which are considered to be very important properties of any paper.

Correspondence to: O. J. Danella, Jr. (sati@power.ufscar.br).

Journal of Applied Polymer Science, Vol. 88, 2346–2355 (2003)

TABLE I
Granulometric Distribution of the $CaCO_3$ Inacarb 700

Cumulative percentage by weight	Diameter (μm)
10	2.6
30	5.2
50	8.5
70	12
90	18
100	—

Besides the formation of microcativities, other surface modifications and surface irregularities are very important characteristics in the improvement of printing quality.[14] Among all of the physical and chemical surface treatments applied to the films, the three most often used are corona discharge, surface etching methods, and the addition of polar polymers in the composition of the films.[3,4,14,17–19] These modifications increase the polar component of the surface free energy (γ_s^p) and, by doing so, also increase the ability of polar inks to be printed on the films.

However, the roughness of any surface of any material affects the contact angles (θs) of certain liquids when applied to that surface, which means that the larger the size of the crevices on the surface is, the smaller the θs under the same conditions of analysis are.[14] Therefore, films with more irregular surfaces have higher values for total surface free energy (γ_s), which creates better ink absorption and adhesion. This is just as true for polar ink as it is for apolar ink because of the increase of the surface area of the film and other factors, such as porosity and the presence of capillaries. The filler particles, and even corona discharge treatment,[14] can result in an increase in the surface irregularity of the films and can, therefore, increase printing quality and ink adhesion.

The control of film surface properties through the physical or chemical modifications mentioned previously can improve ink absorption and adhesion on synthetic paper. Controlling the dispersion and distribution of both filler particles and controlling the blend phases of immiscible polymers contribute to the enhancement of the printing quality on synthetic film papers because of the uniformity of all the film properties.

EXPERIMENTAL

Materials

The polymers used in this study were PP (RF6100, Polibrasil Resinas S. A., Mauá, Brazil) and PS (Polystyrol 148G, BASF, São José dos Campos, Brazil) with melting indices of 8.0 and 6.0 g/10 min, respectively.

As the compatibilizer, PP-*g*-PS was used, which was produced in the Materials Engineering Department laboratories at the Federal University of Sao Carlos (Sao Carlos, Brazil),[20] and as antioxidants, B 215FF and PS 802 FL (Ciba, São Paulo, Brazil) were used. The fillers were natural calcium carbonate Inacarb 700 (Quimbarra, Mogi das Cruzes, Brazil), titanium dioxide (Cardinalli Indústria e Comércio, Ltd., São Carlos, SP, Brazil), and silicon (Syloblock 44, Grace Davison, Sorocaba, Brazil) with a purity of 99%. All of these materials were used as received without any further treatment.

Table I shows the granulometric distribution and the average particle size of the Inacarb 700 calcium carbonate.

For all of the tests that we carried out on the synthetic paper films, a cellulosic paper made for printing was used as a reference (Xerox do Brasil, São Paulo, Brazil).

Film processing

Table II shows the mass of the components for each of the five formulations used in this study. The quantities showed for SiO_2, TiO_2, PP-*g*-PS, and the antioxidants are related to parts per hundred of the PP/PS/$CaCO_3$ composite.

All of the raw materials of each film were initially mixed in a Werner-Pfleiderer (New Jersey) twin-screw extruder coupled with two vibrating feeders at a screw speed of 200 rpm. The temperatures of the six zones in the extruder were 190, 220, 235, 240, 240, and 240°C. The fillers were introduced into the melt-flow polymers in the melting zone. The extrudate was cooled in water at room temperature, cut into pellets, and then dried at 80°C in a vented oven for 6 h. Before processing, the calcium carbonate was dried at 100°C for 12 h.

The synthetic paper films were obtained with a single-screw flat-die extruder (Imacom EMR 25 mm,

TABLE II
Synthetic Paper Films Processed in a Werner-Pflaiderer Extruder

	PP	PS	$CaCO_3$	TiO_2	SiO_2	PP-*g*-PS	Antioxidant
C1	60	40	0	3	1	5	0.10
C2	60	0	40	3	1	0	0.10
C3	60	20	20	3	1	5	0.10
C4	60	10	30	3	1	5	0.10
C5	75	0	25	1	1	0	0.10

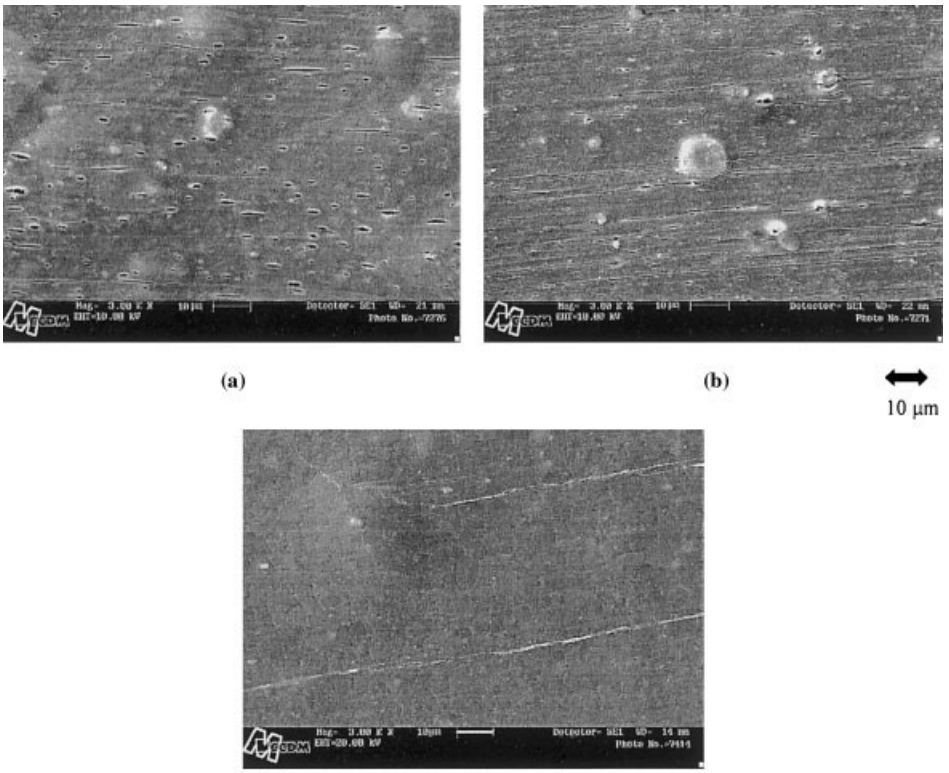

Figure 1 Scanning electron micrographs of the surface of film C1 (3000×): (a) SRm, (b) SRh, and (c) nonetched.

São Bernardo do Campo, Brazil; length/diameter ratio = 30). The temperatures of the five zones in the extruder were 200, 200, 210, 220, and 220°C at a screw speed of 200 rpm.

After processing, the films were stretched at two different rates, which are referred to as the high stretching rate (SRh) and the minimal stretching rate (SRm). The exact values of the stretching rates were not determined, but these same conditions were applied to all the films. The temperature during stretching was fixed at 155°C.

After stretching, the films were submitted to corona discharge treatment on the rougher side of the film.

Scanning electron microscopy (SEM)

A Leica Estereoscan 440 scanning electron microscope (Cambridge, UK) was used to study the surfaces of all the films. The films were covered in gold before they were examined under the microscope at an acceleration voltage of 10 kV. To provide better insight into the morphology of the films with PS in their composition, we etched these samples with tetrahydrofuran (C_4H_8O) at room temperature for 24 h.

Friction coefficient analyses

The coefficients of kinetic and static friction were calculated for all of the film samples with the ASTM D 4917-89 method. A specific instrument with horizontal sheets was used for the test, in accordance with this standard.

γ_s

A Ramé-Hart 100-10goniometer (New Jersey) was used to measure the θs of the film surfaces with three different liquids: water and diethylene glycol were used on cellulosic paper, and water and methylene iodide (CH_2I_2) were used on synthetic film papers. The substitution of methylene iodide for diethylene glycol in cellulosic paper was necessary because the former instantaneously spread out on the cellulose surface when applied to the paper. The values of these angles were correlated to the γ_s of the films according to Young–Dupré and on the basis of the reciprocal mean and force additivity :

$$\gamma_{SL} + \gamma_{LV}\cos\theta = \gamma_{SV} \quad (1)$$

$$\gamma_{SL} = \gamma_{LV} + \gamma_{SV} - 4\left(\frac{\gamma_s^d\,\gamma_L^d}{\gamma_s^d + \gamma_L^d} + \frac{\gamma_s^p\,\gamma_L^p}{\gamma_s^p + \gamma_L^p}\right) \quad (2)$$

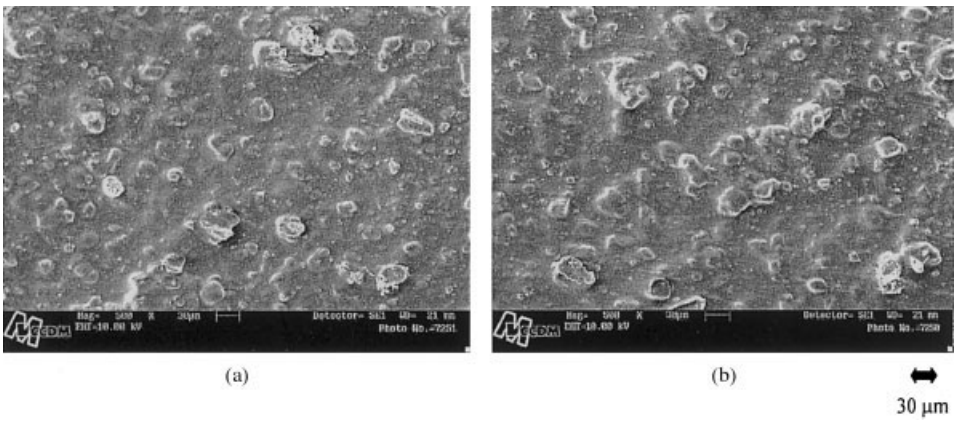

Figure 2 Scanning electron micrographs of the surface of film C2 (500×): (a) SRm and (b) SRh.

where γ_{SL} is the interface tensile between solid and liquid, γ_{LV} is the interface tensile between liquid and gas, γ_{SV} is the surface free energy of the solid, γ_s^d is the chromatic dispersion component of the solid, γ_s^p is the couple pole or polar component of the solid, γ_L^d is the chromatic dispersion component of the liquid, and γ_L^p is the couple pole or polar component of the liquid.

The θ used for the γ_s analyses was obtained from the average of 10 measurements from each film. The temperature and relative humidity were fixed at 25 ± 2°C and 60%, respectively.

Ink absorption

All of the samples of cellulosic and synthetic film papers were weighed before and after the application and drying of a thin layer of offset ink. Initially, five samples from each film with an area of 144 cm^2 were weighed. Afterward, a thin layer of offset ink was evenly applied over the entire surface of the films. All of the excess ink was carefully removed from the films, and then, the paper and ink together were weighed. The ink absorption was calculated by the calculation of the difference in the weight of the paper with ink on it and the weight of the paper by itself. The temperature during the tests was kept at 23 ± 2°C, and the relative humidity was fixed at 60%.

Ink adhesion

Ink adhesion was calculated for the all of the samples with ASTM D 3359-90. A specific type of tape was used for the adhesion analyses; it was applied with a constant force during the entire process. We then examined, with qualitative analyses, how much ink adhered on the film surfaces by pealing the tape off of the films.

RESULTS AND DISCUSSION

SEM observations

Obtained with a scanning electron microscope, Figures 1 to 5 show the film surfaces of the synthetic paper films at the two different stretching rates for each film, SRh and SRm. The films in Figures 1, 3, and

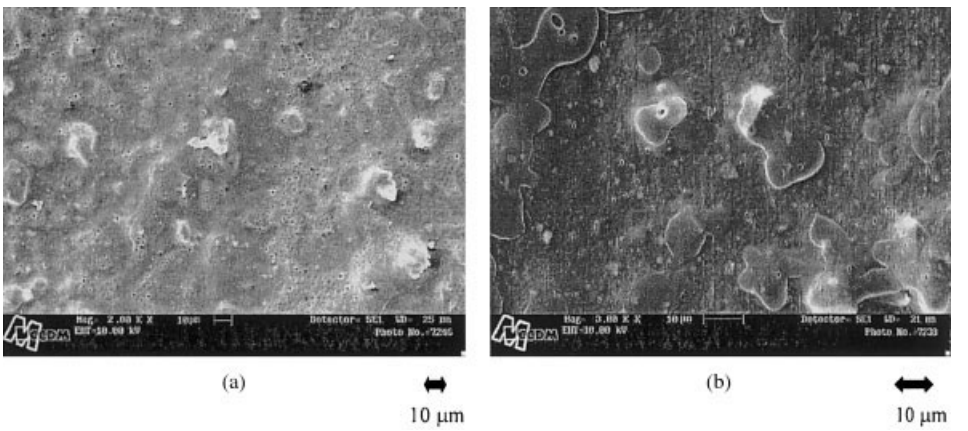

Figure 3 Scanning electron micrographs of the surface of film C3: (a) SRm (2000×) and (b) SRh (3000×).

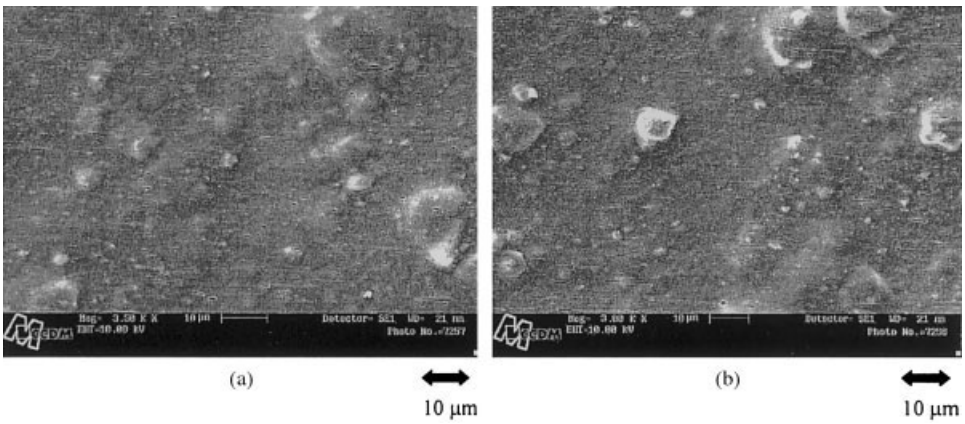

Figure 4 Scanning electron micrographs of the surface of film C4: (a) SRm (3500×) and (b) SRh (3000×).

4 were etched with tetrahydrofuran (C_4H_8O). Figure 1(c) shows a nonetched film for comparison.

Even though the rates of stretching were not quantitatively calculated, one can see in the micrographs that significant differences existed in the orientation of the films in relation to the two rates of stretching, which showed a larger orientation at SRh. Films C1, C3, and C4 better represented this effect, being the only ones with PS in their compositions. The crevices shown in Figure 1(a,b) represent the removed PS phase before analysis. This is confirmed by the film shown in Figure 1(c), where the nonetched film showed no development of cavities or voids. These same films also showed both good dispersion and control of the average sizes of the domains of PS. This, in turn, indicated good interaction between the PP and PS phases during the processing of the films. This behavior was mainly due to the use of the PP-*g*-PS copolymer, which acted as a compatibilizing agent in the PP/PS blend, thus decreasing the interfacial tension and facilitating the interaction and transference of tension between the phases of the blends.[21] The PP-*g*-PS copolymer, according to Adewole et al.,[22] has a high capability of acting between the PP and PS interfaces, decreasing the interfacial tension and, consequently, the average size of the domains of the dispersed phase. More over, this copolymer can stabilize the morphological structure of the blend during and after manufacturing. At the SRh for films C1, C3, and C4, a longer stretching of the PS phase was observed in relation to the SRm, resulting in a greater stretching tension at the SRh and a good transference of tension between the blend phases, both due to use of the compatibilizing agent.[21]

According to the total quantities of PS in films C1, C3, and C4, as shown in Table II, the film C1 had a larger amount of PS in its compositions, which therefore resulted in a larger PS phase when compared to films C3 and C4, which had less PS in their compositions. Figures 1, 3, and 4 demonstrate this effect.

As shown in Table II together with Figures 1–5, the increase in the amount of $CaCO_3$ in the film brought about an increase in the surface irregularity of the films. This was demonstrated in films C2, C4, and C5, which had large quantities of $CaCO_3$ and which, therefore, presented the highest amount of surface irregularities.

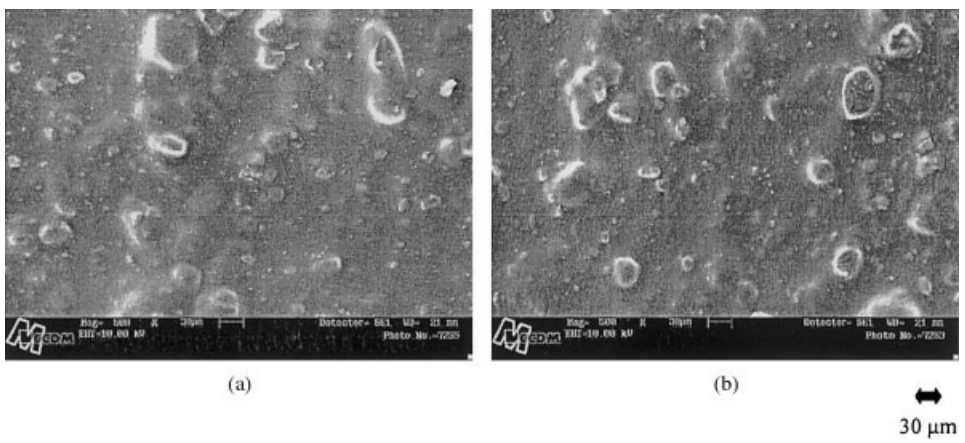

Figure 5 Scanning electron micrographs of the surface of film C5 (500×): (a) SRm and (b) SRh.

TABLE III
Coefficient Values for Both the Static and Kinetic Frictions of the Samples

Sample	Stretching rate	Static coefficient	Kinetic coefficient
	SRm	0.430	0.422 ± 0.019
C1	SRh	0.413	0.394 ± 0.014
	SRm	0.561	0.546 ± 0.016
C2	SRh	0.537	0.522 ± 0.010
	SRm	0.439	0.400 ± 0.015
C3	SRh	0.423	0.394 ± 0.009
	SRm	0.552	0.434 ± 0.019
C4	SRh	0.542	0.444 ± 0.023
	SRm	0.541	0.506 ± 0.018
C5	SRh	0.538	0.472 ± 0.007
Cellulosic paper	—	0.320	0.291 ± 0.015

There was no development of microcavities on the surfaces of the synthetic film papers, in agreement with what was observed in the micrographs. The observed cavities seen in films C1, C3, and C4 were caused by the PS phase etched by THF. Most likely, the set rates in the uniaxial orientation process of the films, the temperature, and the two rates of stretching were not all ideal for the successful formation of the microcavities. Furthermore, the large average size and distribution of the $CaCO_3$ particles used in the films (Table I) could have impaired the development of the microcavities. In fact, for better development of microcavities, the ideal distribution of the filler particles should fall within the range 0.05–8 μm, according to some authors.[3–5] New studies are currently being carried out, which are aiming to obtain microcavities on the film surfaces.

Friction coefficient

Table III supplies the data for the static and kinetic frictions for all of the synthetic film papers at the two stretching rates, SRh and SRm. For the values of the kinetic friction coefficient, the standard deviation was calculated.

As shown in Table III, films C2, C4, and C5 had higher values for static friction when compared to films C1 and C3. In agreement with Figures 1–5, this

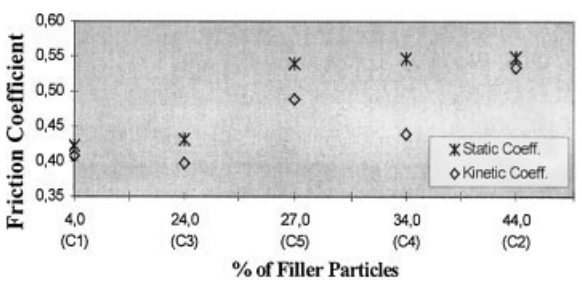

Figure 6 Comparison of the coefficient values for static and kinetic friction related to the quantity of filler particles.

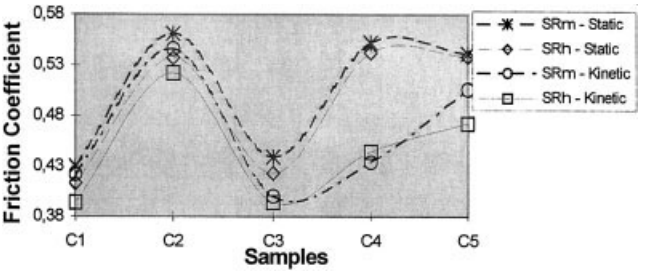

Figure 7 Comparison of SRh and SRm in relation to the static and kinetic coefficients.

was related to higher surface irregularity, which was due to larger quantities of filler particles, mainly $CaCO_3$, in their formulas. The kinetic friction coefficient showed similar behavior to that of the static friction, both showing higher values for C2, C4, and C5 when compared to those of the other films. The only difference was that the kinetic friction had smaller values compared to static friction.

Figure 6 shows the behavior of the static and kinetic friction coefficients in relation to the mass of the filler particles for each film (Table II). These values are shown in terms of filler percentages, calculated from the average of the stretching rates of the films, the SRh and SRm.

The greater values of the static friction coefficient in relation to the kinetic friction coefficient are clearly shown in Figure 6 for all of the samples. Furthermore, the higher values for the friction coefficients can be observed for films C2, C4, and C5 with the higher quantities of calcium carbonate in their compositions.

Figure 7 shows the relationship between SRh and SRm and the static and kinetic coefficients.

This figure clearly shows the differences between the static and kinetic friction coefficients. As also shown in this figure, the SRh had a tendency to reduce the static and kinetic friction coefficients when compared to the SRm. This could be associated with the greater stretching of the polymeric matrix at the SRh, which decreased the surface irregularity, which in turn decreased the area of contact between the films during the friction test and, therefore, reduced the friction between them. Despite this, there were no significant differences in relation to the type of film processing used in terms of greater (SRh) or lesser (SRm) stretching in relation to the variations of the static and kinetic friction coefficients for the films.

Analysis of the surface energy

Table IV shows the surface energy values for all of the synthetic film papers at both SRh and SRm when the corona discharge treatment was applied to the rougher side of the films. Furthermore, γ_s values were analyzed for both the synthetic paper film and for

TABLE IV
Surface Energy Values for Synthetic Film Papers, Cellulosic Paper, and Pure PS

Sample	θ (H_2O)	θ (CH_2I_2)	$\gamma^d s$ (mN/m)	$\gamma^p s$ (mN/m)	γ_s (mN/m)
C1					
SRm	97.83 ± 2.64	41.86 ± 2.98	38.7	2.6	41.3
SRh	95.86 ± 2.30	46.00 ± 1.89	34.8	3.0	37.8
C2					
SRm	94.11 ± 1.88	39.29 ± 1.67	43.7	1.7	44.4
SRh	94.21 ± 2.04	33.50 ± 2.93	41.8	2.5	44.3
C3					
SRm	95.10 ± 2.27	48.69 ± 3.21	32.6	3.7	36.3
SRh	95.50 ± 1.52	45.93 ± 2.15	34.6	3.2	37.8
C4					
SRm	94.84 ± 1.17	43.92 ± 1.15	34.8	3.7	38.5
SRh	96.30 ± 2.68	46.50 ± 2.35	34.8	2.8	37.6
C5					
SRm	90.80 ± 1.38	40.50 ± 1.73	40.8	2.7	43.5
SRh	92.70 ± 0.80	34.90 ± 1.33	39.7	2.3	42.0
PS					
SRm	77.29 ± 5.84	37.58 ± 4.13	32.1	11.1	43.2
SRh	77.92 ± 3.86	32.43 ± 3.74	34.5	10.3	44.8
Paper[a]					
—	62.40 ± 2.9	26.60 ± 1.70	21.7	22.7	44.4

[a] The values for θ with regard to cellulosic paper were calculated in relation to water and diethylene glycol.

pure PS, which was the same PS used in the synthetic film papers and which was also processed under the same conditions as the synthetic film papers.

As shown in Table IV, films C2 and C5 had the highest γ_s in relation to the other synthetic film papers and came close to the values for that of cellulosic paper. However, cellulosic paper had such a high value because of the γ_s^p in its γ_s in relation to the other synthetic film papers. This was due to both the high polarity of the cellulose fibers and to the several surface treatments carried out on the cellulosic paper.[14,16]

For films C2 and C5, however, the high values of γ_s were not caused by the polar component but rather by a high γ_s^d of the γ_s. The smaller polarity and the greater roughness of the synthetic paper films in relation to cellulosic paper, especially for films C2 and C5, in some way could have assisted the γ_s^d's to reach these higher values. It is known that rougher surfaces of a solid have smaller θs between a drop of liquid and their surfaces than those formed with smoother surfaces.[14] Therefore, with a smaller θ, it is common to expect greater γ_s of any solid, according to the Young–Dupré equation . This may have influenced the synthetic film papers, notably, C2 and C5 (the rougher films), to achieve higher values of γ_s^d, thus increasing γ_s.

Figure 8(a,b) shows the θs for both water and methylene iodide in relation to the increase in the percentage of filler particles and, consequently, for the level of surface irregularity of the films.

As shown in Figure 8(a,b), there was a tendency for the θs of both water and methylene iodide to decrease as the surface irregularity of the films increased, mainly for methylene iodide. Furthermore, Figure 8(a,b) shows no significant differences in the θ measurements at both SRh and SRm. This aspect indicates that the two stretching rates used in this study, SRh and SRm, did not affect the irregularity of the film surfaces in a significant way.

As shown by the γ_s^p values in Table IV, all the synthetic film papers presented a certain surface po-

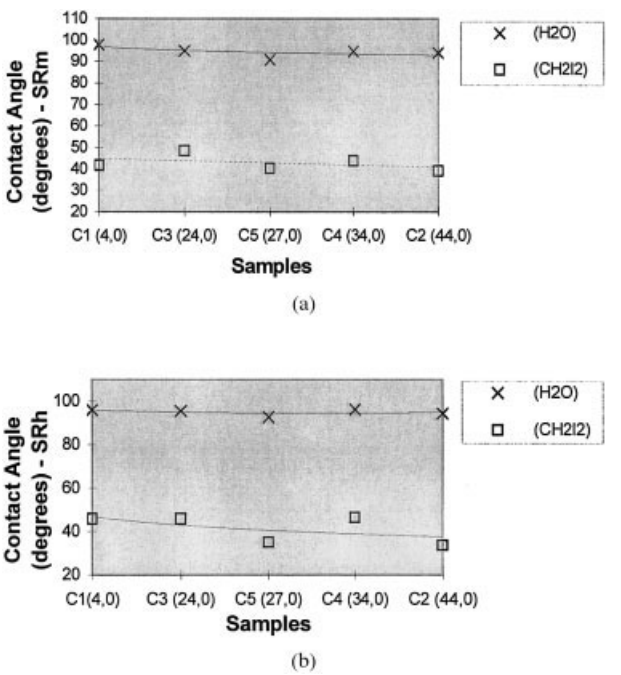

Figure 8 θs for water and methylene iodide in relation to the percentage of all inorganic fillers of the films at both SRh and SRm.

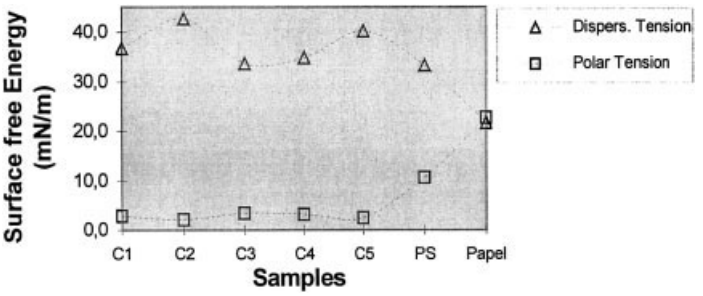

Figure 9 γ_s divided into γ_s^p and γ_s^d for all of the films.

larity, which was probably due to the corona discharge applied on them. However, for films C1, C3, and C4, which had PS in their formulas, a slight increase was observed in γ_s^p when compared to films C2 and C5.

Figure 9 illustrates the γ_s values for the synthetic film papers and for pure PS. The values in the chart refer to the average value for γ_s with both rates, SRh and SRm, considered.

The largest values of γ_s^p for the pure PS films indicated that this polymer influenced the level of surface polarity for films C1, C3, and C4, which all had PS in their formulas.[3] Furthermore, Figure 9 clearly demonstrates the elevated values of the γ_s^d in the surface energy for the films by showing a high concentration of $CaCO_3$, namely, in films C2, C4, and C5.

Figure 10 shows, in more detail, the influence of PS on the increase of γ_s^p in the γ_s of synthetic film papers and in pure PS. Again, the values in this chart refer to the average values for the γ_s^p with both rates, SRh and SRm, considered.

As shown Figure 10, among all of the synthetic film papers, films C1, C3, and C4 had higher surface polarities. Further, the PS helped to increase these polar components because the pure PS film had greater values of γ_s^p in relation to the other films, which resulted in smaller concentrations of PS in their compositions.

Besides film C1 having a higher quantity of PS compared to films C3 and C4, it also presented smaller values for γ_s^p. One possible reason for this behavior was that the composition of the film included smaller values of PP-*g*-PS in relation to PP/PS in the blend C1 (Table II). Moreover, this is what could have been influenced in the morphology and in the interface properties of the immiscible phases of the blends, influencing the θ measurements and the total γ_s.

Offset ink absorption

Figure 11 shows the results of absorption of the offset ink for all the synthetic papers at SRh and SRm. As shown in this figure, films C2, C4 and C5 stood out in the absorption of the offset ink, presenting greater values at both SRh and SRm.

According to previous analyses, films C2, C4, and C5 presented larger values for the friction coefficient and γ_s (mainly C2 and C5). The higher surface irregularity of these films could have influenced the rise in γ_s and, because of this, caused an increase in the absorption and/or adhesion of the offset ink. The greater surface irregularity of these films influenced the increase in surface area, therefore causing a larger contact area between the ink and the film, resulting in higher offset ink absorption.[14] Also, the offset ink had apolar characteristics because it had long chains of soybean oil in its basic alkydic chemical structure.[23] These specific characteristics increased absorption and/or ink adhesion of the films that were less polar, namely, C2 and C5.

For films C1 and C3, low absorption was observed, mainly for C1, in comparison to the other films. In addition to the films having lower surface irregularity, the use of PS in the formulas for these films increased

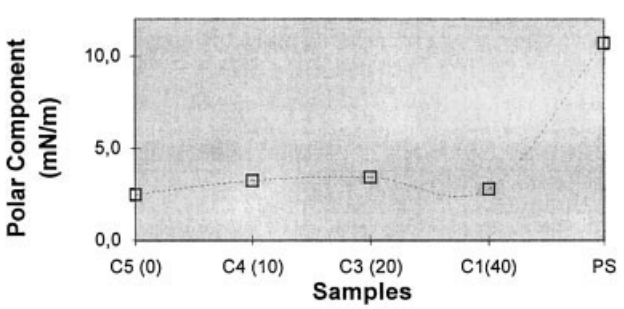

Figure 10 γ_s^p for all of the synthetic paper films and for pure PS.

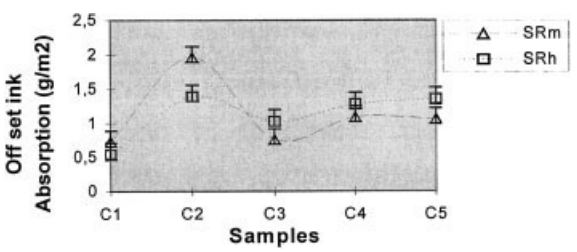

Figure 11 Offset ink absorption (g/m^2) for the synthetic film papers at SRh and SRm.

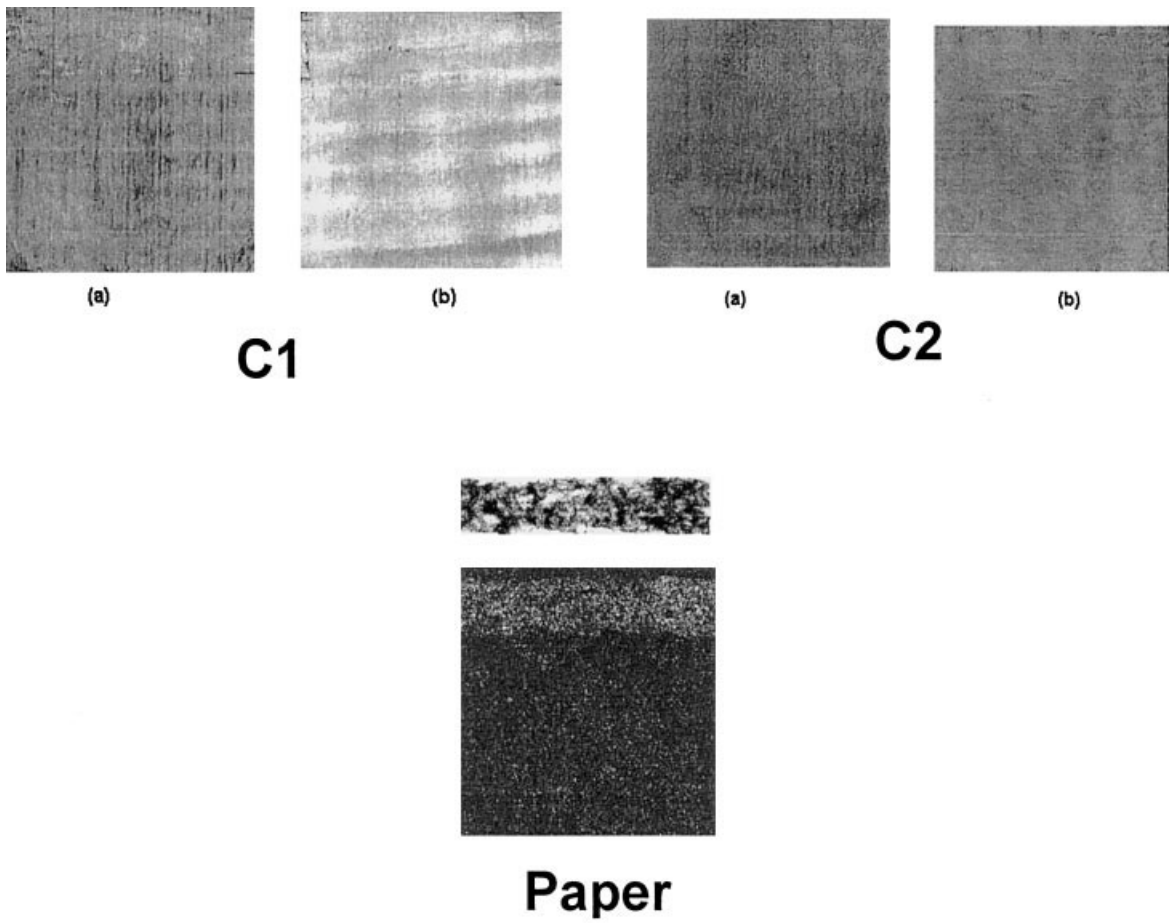

Figure 12 Adherence for the synthetic film papers C1 and C2 and for cellulosic paper.

their polarity, which decreased their offset ink absorption.

The cellulosic paper absorbed substantially more ink than the synthetic film papers, reaching values close to 15 g/m^2, which is not shown in Figure 6. This behavior of the cellulosic paper in relation to the synthetic film papers was due to its high fibrilar structure and porosity. Furthermore, specifically applied treatments during its production, such as the incorporation of filler particles and surface treatments, may have improved the absorption and rapid drying of the ink.[14,16]

Analysis of the adherence of offset ink on the paper

Figure 12 shows the results of the adherence test on synthetic film papers C1 and C2 and on cellulosic paper. Figures 12(a) and 12(b) for films C1 and C2 correspond to the SRm and SRh, respectively. The remaining films are not shown because they presented ink absorption characteristics that were neither high nor low but fell rather within the two extremes represented by C1 and C2.

The stronger tonality of the offset ink when used on cellulosic paper proved its great absorption. As also shown in Figure 12, film C2 presented a strong tonality in relation to film C1, which was in agreement with the previous results for the friction coefficients, γ_s, and ink absorption. As shown in this figure, the SRm showed a slightly stronger tonality of ink when compared to SRh, indicating a greater absorption. The larger friction coefficients for SRm contributed to this behavior, according to the facts in Figure 7, which shows the high influence of the irregularities on the film surfaces on ink absorption. Even though the difference in surface irregularity between SRm and SRh was not so large (Fig. 7), there was an obvious variation in its effect on ink absorption.

With relation to the offset ink adhesion of synthetic film papers, C2 also presented a high level of adherence. This aspect could be observed either on the film surface, which showed fewer parts left in white in the test region, or on the transparent tape that was peeled off, which showed a lower quantity of ink removed. This was caused by a greater level of irregularity on

the surface of film C2, which seems to be the most important characteristic of the film with regard to increasing the difficulty with which the offset ink is removed. Furthermore, film C2 had a greater affinity with the offset ink, showing less surface polarity.

Interestingly, in addition to the cellulosic paper showing higher levels of ink absorption, a large amount of ink was also removed from it. The removal of the cellulose fibers from the surface with adhesive tape was largely responsible for this. This is one of the advantages of synthetic film paper over cellulosic paper: the synthetic film paper does not demonstrate this behavior.

CONCLUSIONS

The control of the surface properties of the films, such as by corona discharge treatment; the addition of polar polymers such as PS to the film compositions; and also surface irregularities are all fundamental for increasing ink absorption. Depending on the characteristics of the ink, polar or apolar, one or more of the aforementioned treatments or properties may be more effective than the others.

In this study, the use of PS in the film compositions increased the polarity and decreased the surface irregularity of the films, impairing offset ink absorption and adhesion, because of both the apolar characteristics of the offset ink used and the minimal contact area between the ink and the films that had PS in their compositions.

However, the increase in the quantity of filler particles caused an increase in irregularity on the film surface, thus increasing the static and kinetic friction. This, in turn, decreased the θ between the drops of liquids and the surfaces, and this increased the γ_s. These factors resulted in the greater absorption and adhesion of the offset ink on the rougher film papers, which were the film papers with larger quantities of filler particles and without PS in their compositions.

Films stretched at SRm showed slightly greater ink absorption than those stretched at SRh, which was due to larger coefficients of both static and kinetic friction, and this was probably a result of the higher surface irregularity of the films at SRm.

References

1. Associação Nacional dos Fabricantes de Papel e Celulose; Celulose e Papel: São Paulo, Brazil, 1999, 15(64).
2. Associação Nacional dos Fabricantes de Papel e Celulose; Celulose e Papel: São Paulo, Brazil, 1996, 8(55).
3. Mannar, S. M. Eur. Pat. 0605938 A1 (1994).
4. Ohno, A.; Goseishi, O. Y. Eur. Pat. 0685331 A1 (1995).
5. Henbo, M.; Hirabe, T. Eur. Pat. 0796730 A2 (1997).
6. Johnston, G. Eur. Pat. 95/16575 (1995).
7. Allen, F. L. U.S. Pat. 05552011 (1996).
8. Huang, H. W. Eur. Pat. 0773094 A1 (1995).
9. Desai, S. C. Pop Plast Package 1994, 39(11), 45.
10. Paper Film Foil Conv. USA 1995, 69(2), 28.
11. Plast. Ind. News, Japan, 1994, 40(5), 69.
12. Plast. Ind. News, Japan, 1994, 40(11), 150.
13. Lin, A.; Taipei, T. W. U.S. Pat. 6001290 (1999).
14. Miller, M. L. Encyclopedia of Polymer Science and Technology; Interscience: New York, 1964; Vol. 1.
15. Manrich, S.; Agnelli, J. A. M. J Appl Polym Sci 1989, 37, 1777.
16. Kline, J. E. Paper and Paperboard: Manufacturing and Converting Fundamentals; Miller Freeman: CA, 1982.
17. Fonseca, C.; Perena, J. M.; Fatou, J. G.; Bello, A. J Mater Sci 1985, 1, 3283.
18. Garby, L.; Charbert, B.; Sage, D.; Soulier, J. P. Angew Makromol Chem 1995, 2, 73.
19. Pinto, G. V. V.; Abreu, C. M.; Knoechelmann, A.; Almeida, Y. M. In 5th Brazilian Polymer Congress, Águas de Lindóia: Brazil, 1999; p 436.
20. Manrich, S.; Rosalini, A. C.; Danella, O. J., Jr. (to Federal University of São Carlos). Brazil Pat. Deposit PI 9907568-7 (2000).
21. Paul, D. R.; Newman, S. Polymer Blends; Academic: New York, 1978; Vols. 1 and 2.
22. Adewole, A. A.; DeNicola, A.; Gogos, C. G.; Mascia L. Plast Rubber Compos 2000, 29, 70.
23. Deutch, P.; Fazenda, M. R. J. In Tintas e Vernizes, 2nd edition; Texto Novo Ed. e serviços Ltda.: São Paulo, Brazil, 1995; Vol. 1.